



# Data-Based Model Parametrization of Quality Predictive Material Removal Simulations

Matthäus Loba<sup>(✉)</sup>, Christian Brecher, and Marcel Fey

Laboratory for Machine Tools and Production Engineering (WZL), RWTH Aachen University,  
Steinbachstraße 19, 52074 Aachen, Germany  
m.loba@wzl.rwth-aachen.de

**Abstract.** The ability to control product quality in milling processes is an essential target variable. Quality deviations can have different causes, which can be both systematic and stochastic. Tracing data from numerous sensors of modern machine controls and combining them with a material removal simulation (MRS) allows to predict the workpiece quality in a process-parallel manner. The accuracy of the prediction depends on the underlying model and its parametrization. Model parametrization usually requires measurements during which the machine tool cannot be used. Additionally, the necessary measuring equipment is often not available in companies. All this makes the implementation of MRS difficult in the manufacturing industry. This article presents an approach that circumvents the abovementioned disadvantages. With the help of a MRS, machine data is refined and contextualized with quality data. The refined and contextualized data is then used to fit various models, such as stiffnesses and process force. In future the presented approach should enable a cost-effective parametrization without machine downtime. With the parameterized models, MRS that predict quality can be used both in advance during CAM planning and in a process-parallel manner for quality monitoring.

**Keywords:** Machine Data Analysis · Process Modelling · Model Parametrization

## 1 Introduction

During machining, different effects occur which influence workpiece quality, productivity and availability of the tools and the machine (e.g. due to wear). During process planning, these three parameters must be optimized to enable an economical production [1]. With regard to productivity and tool wear, tool manufacturers already offer a preselection of optimized parameters. However, the tool manufacturer cannot predict the workpiece quality in its full complexity, since in-depth knowledge, e.g. about the stiffness behavior of the machine tool, is usually necessary. In previous work, the prediction of workpiece quality has been addressed in CAM planning [2] as well as in process monitoring [3]. The prediction accuracy of these simulations depends on the one hand on the discretization and on the other hand on the models behind it. Especially the model parametrization is still very time-consuming and costly, due to the necessary

measurements which have to be performed out of production mode. At the same time, the measurements require special equipment and qualified personell. All these factors lead to the fact that the solutions are currently not used on an industrial level. An approach that uses existing resources and does not disrupt production is therefore necessary.

In this paper, a concept is presented that addresses this challenge. In a first step, the state of the art of modeling certain effects and parametrizing their model is discussed. Subsequently, a concept is presented that enables a model parametrization based on machine and quality data. The procedure of the concept is conducted for separate models. Finally, a summary and an outlook are given.

## 2 Machining Errors

In recent years, numerous models and approaches have been developed along the digital process chain that enable quality prediction in machining. The influences on the workpiece quality can be classified according to different criteria. Apart from the classification according to the degree of order of the defect on the workpiece (cf. [4]), the influences can also be classified according to their source (machine-, workpiece-, tool- and process-related) [5] or the type of generation [6]. When classifying according to the type of generation, it should be noted that some of the influences interact with each other. For example, the cutting edge geometry and its position (tool runout) have an influence on mechanical and thermal factors such as the process force or the heat generation in the process. Altogether, four types of influence are defined: 1) numerical (control) errors, 2) thermal-induced errors, 3) load errors due to a static or dynamic forces and 4) geometric-kinematic errors. In this article, this type of classification is used, since it is considered to be the most useful for the systematic approach of the concept. In addition to [6], the influence of post-processing, the form and location deviation of the raw part and the influence of the clamping force deflection are added.

Mayr et al. state that up to 75% of all geometric defects on the workpiece can be related to thermal influences [7]. In a case study [8], Schmitz investigated the individual influences with regard to effects on the workpiece based on the circle-rhombus-square sample component (NAS979). In the worst case scenario, 76% are due to cutting forces, 18% to geometric and numerical errors, and 6% to thermal expansion of the spindle [8]. Depending on the process parameter setting and running time of the machine, the dimensions can vary [8]. At the same time, the production of the workpiece is a three-axis machining process, so that errors due to post-processing or path errors of the control are rather negligible. Furthermore, the clamping situation is selected in such a way that distortion due to clamping forces tends to be negligible. The variety of workpieces, tools, machine tools, process parameters and environmental influences is so high that the extent of each influence cannot be quantified generally. Rather, this challenge must always be addressed in the context of the entire manufacturing process. In the following, the modeling of the individual errors will therefore be discussed. The focus here is primarily on the model parametrization.

**Numerical errors** can occur due to discretization or miscalculation. They occur mainly in five-axis machining and arise during postprocessing after CAM programming or to the path interpolation of the NC. Both a too high and a too low point density can lead

to machining errors [9]. If the point density is too low, faceting of the surface can occur. If the point density is too high, the feed rate may decrease. The resulting decrease in process force can also lead to machining errors. This can be avoided by continuous-path mode. A disadvantage of this mode is that the programmed contour won't be traversed precisely [10]. As a further numerical error, the interpolation error of the control, which becomes apparent as chord error, should be mentioned [11]. Numerical Errors can be reproduced by using machine-internal data or data from a virtual control (VNCK) [12].

**Thermal-induced errors** are split into two categories. On the one hand, different thermo-elastic expansions occur on the machine side due to heat sources (e.g. power losses of the drives), which influence the machine accuracy. On the other hand, thermal expansions occur in the cutting zone as a result of the cutting energy induced. Most current work in this area uses finite element method (FEM) [5, 8, 13, 14]. Increasingly, however, hybrid approaches are finding an application as they allow faster calculation of the displacements [15]. One way to measure the thermo-elastic machine behavior is presented in [16]. Using position sensing detector sensors and a thermally stable laser frame, 13 out of 21 errors for three-axis machines are detected. In [17], Denkena et al. present a method to model the thermo-mechanical behavior in the cutting zone. By means of a dextral-based material removal simulation (MRS), they calculate the chip cross-section and the resulting forces as well as the generated heat flux. An FE simulation is used to get the actual workpiece expansion, which is stored in the respective dexels. Subsequently, an inverse displacement of the triangulated tool surface is performed.

**Load errors** always dependent on both the forces and torques that occur as well as the interacting stiffnesses.

Existing approaches already allow to predict process forces by means of machine data. In most cases, these are often current based [18] or rely on a prediction based on the difference of the encoders [19]. To parameterize the models, load-deformation curves are used. At the same time, air cuts are run to determine the influence of motion on the correlating variables. At low or reversing velocities these approaches often reach their limits (e.g. due to static friction). In addition, the model parameters are affected by further influences, e.g. due to the running time of the machine and past machining operations, which cannot always be reproduced due to their variance. Hybrid approaches provide an improvement of the prediction accuracy. In [20], Königs et al. use an artificial neural network (ANN) for process-parallel process force estimation. Here, in addition to the machine-internal data, the engagement conditions from the process-parallel MRS are used as input parameters. In [21], Denkena et al. use an ANN with long-short-term memory (LSTM) with motor currents and position data, as well as the variables derived from them, such as axis velocity, acceleration and jerk, as input data for predicting the process force. A disadvantage of approaches for process force prediction using machine data is that dynamic effects cannot be modelled due to the low sampling rate (~500 Hz). Additional sensor technology is required for this purpose. Brecher et al. use a spindle-integrated force sensor (SIFS), which determines the process force via the displacement of the bearing rings [22]. Postel et al. use accelerometers on the main spindle housing to predict the process forces [23]. Furthermore, Denkena et al. use strain gauges on the spindle slide to determine the process force as well as the tool stiffness [24]. All

approaches have in common that in each case the transfer functions between tool center point (TCP) and the sensor locations must be known.

For the prediction of the stiffness at the TCP (tool + machine), FE-based [25] or analytical [26] approaches are mostly used. By means of dynamic substructure coupling, the machine stiffness can also be modeled [25]. In [27], an approach is presented that uses machine and quality data to determine the resulting stiffness. Using machine internal data, a digital shadow is created that stores force information on the part. Based on the shape deviations between the digital and real part, a calculation of the TCP stiffness is performed.

Approaches for modeling the stiffness on the workpiece side deal with both the deformation of thin-walled components [26] due to the occurring process forces and the deformation due to the clamping situation [28]. These approaches are also mostly FE-based.

**Geometric-Kinematic Errors** are all those errors that occur due to the interacting geometries in the load-free state. These errors must be taken into account when modeling the kinematics and the individual geometries. On the workpiece side, these are errors in the raw geometry (e.g. casting allowances) and positioning errors. Machine data can be used to detect tool engagement [29]. This theoretically offers the possibility to predict casting allowances, provided that all other geometries are known. In addition, positioning error can be reduced by continuous calibration of the blanks.

On the machine side, the errors of the individual axes and their position relative to each other should be mentioned. These can be measured both directly and indirectly. A direct measurement can be achieved, e.g. by means of laser measurement systems or double-ball bars. An indirect measurement is possible by the use of specimen workpieces. The individual defects and their measurements are summarized in ISO230 [30].

From tool side, geometric errors are caused by tool runout and tool geometry. Depending on the level of detail of the tool (cf. [31]), different orders of errors can be reproduced. When representing the tool as a hull body, form deviations and the waviness can be modeled. By an additional consideration of the cutting edge geometry a mapping of the roughness of the third order is possible (grooves). The tool geometry is measured in the production scheduling. The individual cutting edge diameters at the TCP as well as the tool runout in the holder can be measured. Clamping in the main spindle causes an additional displacement of the tool rotation axis. At the same time, wear occurs on the tool cutting edges as a result of machining. Schmidt investigated both the calculation of tool runout and cutting edge wear with the help of a force measuring platform [5]. At the same time, there are approaches that use machine data to monitor tool wear [32].

**Conclusion of the State of the Art.** The current state of the art already allows the modeling of many effects. The numerical effects can already be mapped well with the help of VNCK [12]. When considering the errors according to their source, it becomes apparent that geometric kinematic errors on the machine side can be partially recorded by means of specimen workpieces [30]. The modeling of thermal influences on both the machine and the process side is mostly done by means of FE simulations [5, 8, 13, 14, 17]. Variables that influence the process force, such as tool wear or runout, can be predicted indirectly [5]. However, high-frequency force data are often required here.

Controllers, however, offer only low sampling rates, so that the prediction possibilities are limited. Furthermore, a concept to predict tool and machine tool stiffness based on machine and quality data is already available [27].

### 3 Concept

The previous framework for quality prediction can be divided into a real and a virtual part. In real world, the product is first designed in its target geometry and the manufacturing process is planned and prepared. These data are virtually pre-processed to enable process simulation. In practice, this is followed by the production of the product and its quality control. During CNC-Process, data from the machine's internal sensors can be recorded. This data is transferred to a process simulation. Here, together with the pre-processed data, the data is processed within the model chain. In addition to the MRS, typical models describe the machine kinematic or stiffness models of the interacting components (machine, workpiece, tool). At the end of the process simulation, a digital shadow is created. By comparing the real and virtual component, deviations can be determined. These are dependent on the individual models as well as their parametrization. The parameterization takes place only once. By adding an additional parameterization layer, the individual information from the virtual models, the machine data as well as the real and virtual quality data are now connected with each other and a parameter fitting is to be made possible. The entire concept is shown in a simplified form in Fig. 1. Based on this, the procedure will be explained exemplarily in the following for two models.

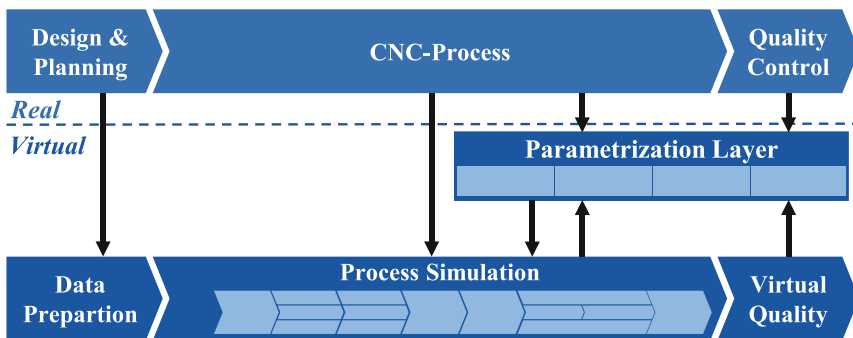


Fig. 1. Data-Based Model Parametrization – Concept

### 4 Data-Based Model Parametrization

For a data-based model parametrization, a deeper analysis of the models and their relationships is necessary. Due to the large number of machining errors, as mentioned in Sect. 2, the procedure will be explained using two examples. One is a process force model and the other is a stiffness model.

In a first step, it shall be assumed that only models describing the ideal state are available. Considering the force model, the resulting current at the main spindle  $I_{Spindle}$  consists of a cutting force component  $I_{cut}$ , and several components related to the spindle position  $s$ , speed  $n$ , acceleration  $a$  and jerk  $j$ . By means of an air cut, these process force-independent components can be recorded so that the linear relationship between cutting force  $F_{cut}$  and the effective cutting edge radius  $r$  of each tool edge and current remains.

$$I_{Spindle} = \underbrace{K_{I,M} F_{cut} \cdot r}_{I_{cut}} + \underbrace{I_j(j) + I_a(a) + I_n(n) + I_s(s)}_{\text{Parameterization based on air cuts}} \quad (1)$$

Kienzle [33] calculate the cutting force for each cutting edge in dependency to the uncut chip thickness  $h$  and width  $b$ :

$$F_{cut,Kienzle,i} = k_{c,i} \cdot b \cdot h^{1-m_{c,i}} \quad (2)$$

The cutting conditions can be calculated with a MRS. Assuming that the force coefficients  $k_{c,i}$  and  $m_c$  are known and constant for a sufficiently long time, the constant  $K_{I,M}$  can be determined by changing the chip thickness or width:

$$K_{I,M} = \frac{\Delta I_{cut}}{\Delta F_{cut} \cdot r} = \frac{\Delta I_{cut}}{\Delta M_{cut}} \quad (3)$$

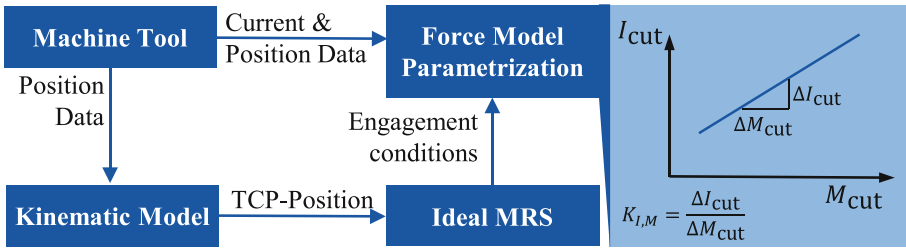
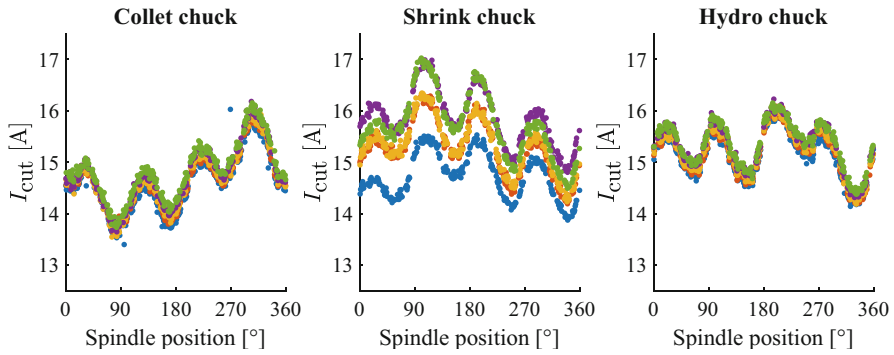


Fig. 2. Force Model Parametrization – Concept

For the determination of  $K_{I,M}$ , it has to be ensured that factors which have an influence on the engagement, e.g. tool runout or tool deflection, are so low that they are negligible. Figure 3 shows the force induced spindle current  $I_{cut}$  during slot milling of C45 with multiple  $\varnothing 16$  mm milling tools (Fraisä Favora P45317610) in different holder types. Each color shows one slot of in different parts. The selected cutting parameters consist of a feed velocity of 525 mm/min, a spindle speed of 2585 rpm, and a cutting depth of 5 mm. For evaluation purposes, a distance of 10 mm was used. It becomes evident that while as  $I_{cut}$  increases over time due to wear, the peaks and valleys remain at a constant spindle position. Based on the extrema, therefore a prediction of the cutting edge location is possible. Afterwards, the chip thickness can be calculated.

Using Eq. 2,  $F_{cut}$  is predicted. Here, the values  $k_{c,i}$  and  $m_c$  are taken from [34]. Based on  $F_{cut}$   $M_{cut}$  is calculated and  $K_{I,M}$  is fitted. The result for one slot is shown in



**Fig. 3.** Force induced spindle current  $I_{\text{cut}}$  during slot milling

Fig. 4. Besides, all results are in Table 1 summarized. The reciprocals of  $K_{I,M}$  can now be used to calculate  $F_{\text{cut}}$  during machining. Besides, further factors, which are related to the force signals, can be calculated. Tool runout can be determined by observing force oscillations, and tool wear by the increase of cutting force coefficients [5]. For the determination of further geometric-kinematic errors, ISO230 can be used [30].

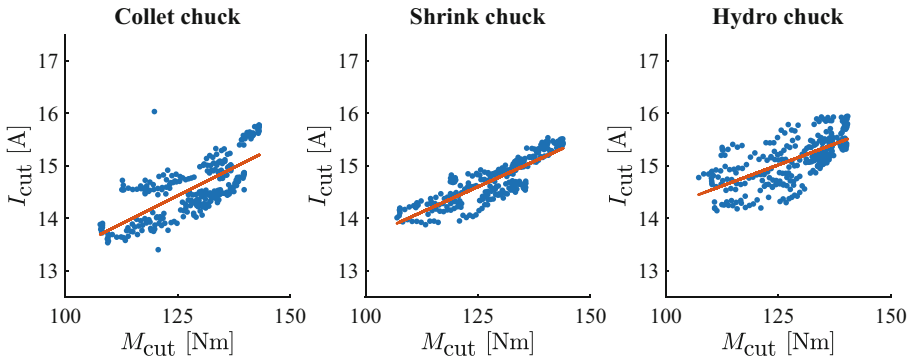


**Fig. 4.** Force Model Parametrization – Results

**Table 1.** Force Model Parametrization – Results

	● Part 1	● Part 2	● Part 3	● Part 4	● Part 5	Mean
<b>Collet Chuck</b>	0.0427 A/Nm	0.0430 A/Nm	0.0431 A/Nm	0.0437 A/Nm	0.0430 A/Nm	0.0431 A/Nm
<b>Shrink Chuck</b>	0.0387 A/Nm	0.0476 A/Nm	0.0463 A/Nm	0.0502 A/Nm	0.0549 A/Nm	0.0476 A/Nm
<b>Hydro Chuck</b>	0.0320 A/Nm	0.0322 A/Nm	0.0326 A/Nm	0.0324 A/Nm	0.0323 A/Nm	0.0323 A/Nm

To calculate TCP stiffness  $k_{\text{TCP}}$ , a virtual workpiece as described in [27], is generated where all stiffnesses are assumed as infinite. In total, three single stiffnesses are connected

in series: 1) cutting part  $k_{\text{cutting}}$  (cantilever beam), 2) holder part  $k_{\text{holder}}$  (static) and 3) machine part  $k_{\text{machine}}$  (static):

$$k_{\text{TCP}} = \left( k_{\text{cutting}}^{-1} + k_{\text{holder}}^{-1} + k_{\text{machine}}^{-1} \right)^{-1} \quad (4)$$

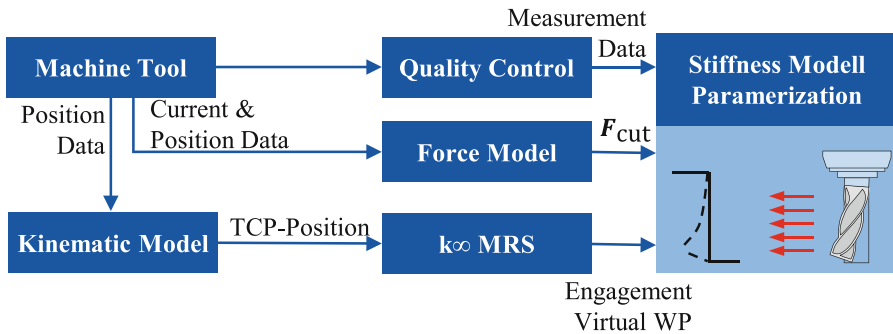


**Fig. 5.** Stiffness Model Parametrization – Concept

The cutting part is modeled as cantilever beam with a uniform load over the cutting depth. By superposing the real and virtual workpiece, the deviation is calculated. Subsequently, the product of Young's modulus and surface moment of inertia is fitted for the cutting edge part. In addition, the holder stiffness together with the machine stiffness is also fitted. By using different tool-holder combinations, the machine stiffness can be extracted later. It should be noted here that the workpiece stiffness is to be neglected. In further work this should be investigated.

## 5 Summary and Outlook

This paper presents a concept that uses machine and quality data to parametrize models for quality prediction. For this purpose, the machine data, which are recorded during the production, are evaluated. Subsequently, individual models are parameterized separately by means of a parameter fitting. The procedure of the concept is described concretely for two models. One is a process force model and the other is a stiffness model. By means of a material removal simulation, the data are brought together in a common context. Here, the engagement variables such as cutting depth and cutting width are determined. By means of a relative analysis, force models can then be fitted. At the same time, the fitted force models can be used to determine other variables, such as tool runout. Furthermore, stiffnesses at the TCP can be determined by superposing digital and real workpiece. In the future, the presented concept can be used to parametrize quality-predictive material removal simulations cost-efficiently during regular production. Therefore this concept can be an enabler for the model parametrization of self-optimizing machining systems as described in [35].



**Acknowledgments.** Funded by the Deutsche Forschungsgemeinschaft (DFG, German Research Foundation) under Germany's Excellence Strategy – EXC-2023 Internet of Production – 390621612.

## References

1. Brecher, C., Epple, A., Fey, M., Königs, M., Neus, S., Wellmann F.: Lernende Produktionssysteme. In: Brecher C, Klocke F, Schmitt R et al. (eds) Internet of Production für agile Unternehmen: AWK Aachener Werkzeugmaschinen-Kolloquium 2017, 18. bis 19. Mai, pp 135–195. Apprimus Verlag, Aachen (2017)
2. Brecher, C., Wellmann, F., Epple, A.: Quality-predictive CAM simulation for NC milling. *Procedia Manuf.* **11**, 1519–1527 (2017). <https://doi.org/10.1016/j.promfg.2017.07.284>
3. Königs, M., Brecher, C.: Process-parallel virtual quality evaluation for metal cutting in series production. *Procedia Manuf.* **26**, 1087–1093 (2018)<https://doi.org/10.1016/j.promfg.2018.07.145>
4. DIN Deutsches Institut für Normung e. V.: DIN 4760:1982–06, Gestaltabweichungen; Begriffe, Ordnungssystem 01.040.17, 17.040.20(4760) (1982)
5. Schmidt, C.: Einflussgrößen-sensitive Simulation und Überwachung von Fräsprozessen. Berichte aus dem IFW. PZH Produktionstechn. Zentrum, Garbsen (2011)
6. Hocken, R.J.: Technology of machine tools. Volume 5. Machine tool accuracy, United States (1980)
7. Schmitz, T.L., Ziegert, J.C., Canning, J.S., Zapata, R.: Case study: a comparison of error sources in high-speed milling. *Precis. Eng.* **32**, 126–133 (2008). <https://doi.org/10.1016/j.precisioneng.2007.06.001>
8. Mayr, J., Jedrzejewski, J., Uhlmann, E., et al.: Thermal issues in machine tools. *CIRP Ann.* **61**, 771–791 (2012). <https://doi.org/10.1016/j.cirp.2012.05.008>
9. Wellmann, F.: Datengetriebene, kontextadaptive Produktivitätssteigerung von NC-Zerspanprozessen, 1st edn. Apprimus Wissenschaftsverlag, Aachen (2019)
10. Siemens, A.G: Programmierhandbuch Grundlagen (2018)
11. Brecher, C., Weck, M. (eds.): Werkzeugmaschinen Fertigungssysteme 3. Springer, Heidelberg (2021)
12. Erkorkmaz, K., Altintas, Y., Yeung, C.-H.: Virtual computer numerical control system. *CIRP Ann.* **55**, 399–402 (2006). [https://doi.org/10.1016/S0007-8506\(07\)60444-2](https://doi.org/10.1016/S0007-8506(07)60444-2)
13. Mayr, J.: Beurteilung und Kompensation des Temperaturganges von Werkzeugmaschinen, ETH Zurich (2009)
14. Vettermann, J., Steinert, A., Brecher, C., Benner, P., Saak, J.: Compact thermo-mechanical models for the fast simulation of machine tools with nonlinear component behavior. at - Automatisierungstechnik **70**, 692–704 (2022). <https://doi.org/10.1515/auto-2022-0029>
15. Brecher, C., Fey, M., Loba, M., et al.: Sustainability in Production Lines. In: Schmitt RH, Bergs T, Brecher C et al. (eds.) Empower Green Production. Conference proceedings, pp 202–232. Fraunhofer-Gesellschaft (2023)
16. Brecher, C., Spierling, R., Fey, M., Neus, S.: Direct measurement of thermo-elastic errors of a machine tool. *CIRP Ann.* **70**, 333–336 (2021). <https://doi.org/10.1016/j.cirp.2021.04.084>
17. Denkena, B., Schmidt, A., Henjes, J., Niederwestberg, D., Niebuhr, C.: Modeling a thermo-mechanical NC-simulation. *Procedia CIRP* **8**, 69–74 (2013). <https://doi.org/10.1016/j.procir.2013.06.067>
18. Aslan, D., Altintas, Y.: Prediction of cutting forces in five-axis milling using feed drive current measurements. *IEEE/ASME Trans. Mechatron.* **23**, 833–844 (2018). <https://doi.org/10.1109/TMECH.2018.2804859>

19. Fey, M., Epple, A., Kehne, S., et al.: Verfahren zur Bestimmung der Achslast auf Linear- und Rundachsen G01L 1/04 (2016)
20. Königs, M., et al.: A scalable, hybrid learning approach to process-parallel estimation of cutting forces in milling applications. *Robert Schmitt Günther Schuh (Publ.)* **7**, 425–432 (2017)
21. Denkena, B., Bergmann, B., Stoppel, D.: Reconstruction of process forces in a five-axis milling center with a LSTM neural network in comparison to a model-based approach. *JMMP* **4**, 62 (2020). <https://doi.org/10.3390/jmmp4030062>
22. Brecher, C., Eckel, H.-M., Motschke, T., Fey, M., Epple, A.: Estimation of the virtual workpiece quality by the use of a spindle-integrated process force measurement. *CIRP Ann.* **68**, 381–384 (2019). <https://doi.org/10.1016/j.cirp.2019.04.020>
23. Postel, M., Aslan, D., Wegener, K., Altintas, Y.: Monitoring of vibrations and cutting forces with spindle mounted vibration sensors. *CIRP Ann.* **68**, 413–416 (2019). <https://doi.org/10.1016/j.cirp.2019.03.019>
24. Denkena, B., Litwinski, K.M., Boujnah, H.: Detection of tool deflection in milling by a sensory axis slide for machine tools. *Mechatronics* **34**, 95–99 (2016). <https://doi.org/10.1016/j.mechatronics.2015.09.008>
25. Albertelli, P., Goletti, M., Monno, M.: An improved receptance coupling substructure analysis to predict chatter free high speed cutting conditions. *Procedia CIRP* **12**, 19–24 (2013). <https://doi.org/10.1016/j.procir.2013.09.005>
26. Agarwal, A., Desai, K.A.: Tool and workpiece deflection induced flatness errors in milling of thin-walled components. *Procedia CIRP* **93**, 1411–1416 (2020). <https://doi.org/10.1016/j.procir.2020.04.101>
27. Loba, M., Brecher, C., Fey, M., Roenneke, F., Yeh, D.-F.: Determination of tool and machine stiffness based on machine internal and quality data. In: Liewald, M., Verl, A., Bauernhansl, T., et al. (eds.) *Production at the Leading Edge of Technology WGP 2022*. LNCS, pp 335–345. Springer, Cham (2023). [https://doi.org/10.1007/978-3-031-18318-8\\_35](https://doi.org/10.1007/978-3-031-18318-8_35)
28. Knappe, S., Königs, M., Epple, A., Brecher, C.: Increasing accuracy of material removal simulations by modeling workpiece deformation due to clamping forces. In: Schmitt, R., Schuh, G. (eds.) *WGP 2018*, pp. 72–80. Springer, Cham (2019). [https://doi.org/10.1007/978-3-030-03451-1\\_8](https://doi.org/10.1007/978-3-030-03451-1_8)
29. Brecher, C., Ochel, J., Fey, M.: Datengetriebene Werkzeugeingriffsdetektion für Fräsprozesse. *Zeitschrift für wirtschaftlichen Fabrikbetrieb* **117**, 784–789 (2022). <https://doi.org/10.1515/zwf-2022-1146>
30. ISO International Organization for Standardization: Test code for machine tools - Part 1: Geometric accuracy of machines operating under no-load or quasi-static conditions 25.080.01(230–1:2012(E)) (2012)
31. DIN Deutsches Institut für Normung e. V.: DIN 4003–1:2017–10, Konzept für den Aufbau von 3D-Modellen auf Grundlage von Merkmalen nach DIN\_4000\_- Teil\_1: Übersicht und Grundlagen 21.020(4003–1:2017–10) (2017)
32. Xi, T., Benincá, I.M., Kehne, S., Fey, M., Brecher, C.: Tool wear monitoring in roughing and finishing processes based on machine internal data. *Int. J. Adv. Manuf. Technol.* **113**, 3543–3554 (2021). <https://doi.org/10.1007/s00170-021-06748-6>
33. Kienzle, O.: Die Bestimmung von Kräften und Leistungen an spanenden Werkzeugen und Werkzeugmaschinen. *VDI-Z.* **94**, 299–305 (1952)
34. Apprigh, T., Brenner, J., Dambacher, M., Dreher, F., Fischer, G., et al.: *Tabellenbuch für Zerspantechnik*. 1st edn. Verl. Europa-Lehrmittel Nourney Vollmer, Haan-Gruiten (2015)
35. Möhring, H.-C., Wiederkehr, P., Erkorkmaz, K., Kakinuma, Y.: Self-optimizing machining systems. *CIRP Ann.* **69**, 740–763 (2020). <https://doi.org/10.1016/j.cirp.2020.05.007>